Journal of Nuclear Medicine, published on April 14, 2022 as doi:10.2967/jnumed.122.263835

Dual-tracer PET/CT protocol with [^{18}F]-FDG and [^{68}Ga]Ga-FAPI-46 for cancer imaging - a proof of concept.

Katrin S. Roth[1], Conrad-Amadeus Voltin[1], Lutz van Heek[1], Simone Wegen[2], Klaus Schomäcker[1], Thomas Fischer[1], Simone Marnitz[2], Alexander Drzezga[1], Carsten Kobe[1]

[1] Department of Nuclear Medicine, Faculty of Medicine and University Hospital Cologne, University of Cologne, Cologne, Germany

[2] Department of Radiation Oncology, Cyberknife and Radiotherapy, Faculty of Medicine and University Hospital Cologne, University of Cologne, Cologne, Germany

Address for correspondence:
Dr. Katrin Roth,
Department of Nuclear Medicine,
Faculty of Medicine and University Hospital Cologne,
Kerpener Str. 62
50937 Cologne,
Germany
E-Mail: katrin.roth@uk-koeln.de

Short title: Feasibility of one-day dual-tracer imaging with [^{18}F]-FDG-[^{68}Ga]Ga-FAPI-46-PET/CT
Key words: Dual-tracer PET/CT, FDG, FAPI
Word-count: 2538

Abstract:

Imaging studies with PET tracers acting as fibroblast activation protein inhibitors (FAPI) show promising results that could usefully complement [^{18}F]-FDG in cancer imaging.

Methods

All patients received [^{18}F]-FDG-PET/CT and dual-tracer PET/CT after additional injection of [^{68}Ga]Ga-FAPI-46 following the [^{18}F]-FDG-PET/CT. Two readers visually compared detection rate and analyzed target-to-background uptake ratios (TBRs) for tumor and metastatic tissue in single and dual-tracer PET/CT.

Results

Detection rate in dual-tracer PET/CT was visually as good as that in single-tracer PET/CT in four patients and superior in two patients, whereas TBRs were significantly higher in dual-tracer PET/CTs.

Conclusion

We demonstrate the feasibility and potential of dual-tracer [^{18}F]-FDG-[^{68}Ga]Ga-FAPI-46-PET/CT administered within a single session. The dual-tracer approach may have superior sensitivity to [^{18}F]-FDG-PET/CT alone without compromising individual assessment of either scan.

Introduction

Fibroblast activation protein (FAP) is a transmembrane glycoprotein, expressed in tissue with activated stroma during wound healing and in chronically inflamed tissue (*1-3*). *In vivo* and histological studies have shown that FAP is also expressed in the tumor microenvironment of human epithelial malignancies (*4,5*). Recent studies with quinolone-based PET radiotracers acting as FAP inhibitors (FAPI) show promising results for [^{68}Ga]Ga-FAPI-46-PET/CT in cancer imaging (*5-7*). Previously suggested advantages of [^{68}Ga]Ga-FAPI-46-PET/CT over [^{18}F]-FDG-PET/CT include fast tumor uptake (*8*) with higher target-to-background ratio (TBR) (*9*). Low background uptake in most organs including brain and liver allows good detection of malignant lesions in these organs by [^{68}Ga]Ga-FAPI-46-PET/CT (*10,11*).

As our knowledge of the clinical impact of FAPI is still incomplete, many therapy strategy decisions for various cancers are currently based on staging with [^{18}F]-FDG-PET/CT, representing the gold standard. Due to tumor-heterogeneity [^{68}Ga]Ga-FAPI-46-PET/CT may not always represent the superior alternative; instead the two tracers may provide complementary diagnostic information. [^{68}Ga]Ga-FAPI-46-PET/CT would therefore often need to be run as a supplement to [^{18}F]-FDG-PET/CT to obtain comprehensive diagnostic information. The aim of the present study was to analyze the feasibility and impact of a single session/dual-tracer PET/CT protocol for cancer staging in patients with head-and-neck tumors (HNT) and esophageal cancer prior to radiotherapy.

Materials and Methods

Dual-tracer protocol

We developed a dual-tracer protocol consisting of an [^{18}F]-FDG-PET/CT (injected activity 272±27.8 MBq, acquisition time 81.3±38.1 min) and a subsequent repeat scan following injection of 177±35.7 MBq [^{68}Ga]Ga-FAPI-46 after a period of 18.2 min±20.1min (Table 1). All patients received first the [^{18}F]-FDG-PET/CT and then the dual-tracer PET/CT after additional injection of [^{68}Ga]Ga-FAPI-46 immediately following the [^{18}F]-FDG-PET/CT-scan.

Patient cohort

Images and data of six male patients who received both an [^{18}F]-FDG-PET/CT and dual-tracer PET/CT with [^{18}F]-FDG and [^{68}Ga]Ga-FAPI-46 between March and June 2021 were retrospectively analyzed. All patients with an average age of 72.5±12.3 years received imaging prior to radio-, chemo- or immuno-therapy. One patient had an inoperable oropharynx carcinoma; one patient with oropharyngeal carcinoma had an additional floor of mouth cancer. Four patients suffered from esophageal cancer (Table 1).

PET/CT-Imaging and -Interpretation

Two independent reviewers visually identified all pathological findings on both single-tracer and dual-tracer PET/CT. The number of lesions and localizations were recorded and compared. CT-scans were used for

correlation and in order to exclude unspecific findings.

TBRs were obtained from both [^{18}F]-FDG-PET/CT and combined [^{18}F]-FDG-[^{68}Ga]Ga-FAPI-46-PET/CT scans by determining ratios of count rates (CR) between suspicious lesions and reference tissue. Maximum CR (CRmax) and peak CR (CRpeak), were obtained within tumor and metastatic lesions by drawing a spherical volume of interest (VOI) around the lesion. Mean CR (CRmean) within reference tissues were measured within a spherical VOI of 2cm diameter in the right liver lobe and within a spherical VOI of 1cm diameter in the cerebellum and mediastinal blood pool (BP).

All procedures were performed according to the regulations of the local authorities (District Administration of Cologne, Germany) and after the local institutional review board (University of Cologne) approved retrospective analysis. This retrospective study was carried out in accordance with the Declaration of Helsinki, with the written consent of all patients to PET/CT imaging and inclusion of their data for scientific analysis.

Statistics

Descriptive statistics were used to present patient characteristics and results. A Wilcoxon matched-pairs signed rank test was performed to check for significant differences between continuous variables. A p-value of less than 0.05 was regarded as statistically significant. Pearson's correlation coefficient was used to measure the strength of the correlation. All statistical analyses were performed using SPSS-Statistics v.27 (IBM, Armonk, NY, USA).

Results

Single-tracer versus dual-tracer protocol

Both single and dual-tracer PET/CT were tolerated well by all patients, without any recorded adverse reactions or side effects. All primary tumors could be clearly detected on [^{18}F]-FDG-PET/CT and [^{18}F]-FDG-[^{68}Ga]Ga-FAPI-46-PET/CT.

In four patients, cervical lymph node (LN) metastases were detected to an equal extent on single and dual-tracer PET/CT (Table 1). In one patient, [^{18}F]-FDG-PET/CT revealed metastasis in only one mediastinal lymph node, whereas [^{18}F]-FDG-[^{68}Ga]Ga-FAPI-46-PET/CT showed tracer accumulation in two additional lymph nodes of the same drainage region. One mediastinal lymph node of a different patient displayed a discrete non-suspicious tracer accumulation on [^{18}F]-FDG-PET/CT but a suspiciously high accumulation on [^{18}F]-FDG-[^{68}Ga]Ga-FAPI-46-PET/CT. [^{18}F]-FDG-PET/CT and [^{18}F]-FDG-[^{68}Ga]Ga-FAPI-46-PET/CT showed an equal extent of pleural metastasis in one patient and a metastasis in the adrenal gland of another patient. [^{18}F]-FDG-[^{68}Ga]Ga-FAPI-46-PET/CT displayed a higher number of liver metastases than [^{18}F]-FDG-PET/CT (n=3-5) in the patient with a metastasis in the adrenal gland (Figure 1).

Whereas [^{18}F]-FDG-[^{68}Ga]Ga-FAPI-46-PET/CT imaging allowed detection of several additional suspicious lesions, no lesions detected on [^{18}F]-FDG-PET/CT were missed in the dual-tracer approach.

Higher mean TBRs in tumors and more metastasis shown on dual- compared to single-tracer PET/CT

As expected, TBRs between tumors and background tissue were consistently higher on combined [^{18}F]-FDG-[^{68}Ga]Ga-FAPI-46-PET/CT compared to single [^{18}F]-FDG-PET/CT (Table 2, Figure 2). The TBRs measured by the Wilcoxon signed-rank test were significantly higher on [^{18}F]-FDG-[^{68}Ga]Ga-FAPI-46-PET/CT than on [^{18}F]-FDG-PET/CT with $z<-2$, p-values ranging from p=0.023-0.008 and strong correlation with $r \geq 0.76$ (Table 2).

TBRs measured between metastases and background tissues were lower in general (Table 2) due to the lower CR of metastatic tissue. The Wilcoxon signed-rank test results were statistically significant with z-values of between -2.35 and -3.06, p-values of $p \leq 0.008$, and a strong Pearson correlation with r ranging from 0.68-0.88 (Table 2).

Unspecific tracer accumulation on dual-tracer PET/CT

Unspecific tracer accumulation was detected in dual-tracer PET/CT around the hip-joint and intramuscular in the flexors of the hip in one patient, evaluated as bursitis or tendinopathy. A pleural tracer accumulation was detected in a different patient most probably caused by scar tissue. An unspecific tracer accumulation was seen in the right femur head and subcapsular in the left liver, most likely as a correlate for reactive processes. In one patient unspecific tracer accumulation was seen in the vein angle (Figure 1).

Discussion

The present study compares dual [^{18}F]-FDG-[^{68}Ga]Ga-FAPI-46-PET/CT with single [^{18}F]-FDG-PET/CT and thereby demonstrates the feasibility and tolerability of dual-tracer PET/CT as well as its potentially higher sensitivity in lesion detection.

Superior diagnostic performance of [^{68}Ga]Ga-FAPI-46-PET/CT compared to [^{18}F]-FDG-PET/CT has been described recently and is mainly attributed to higher TBRs (*9*). We observed an equivalent performance in four patients and diagnostic superiority of [^{18}F]-FDG-[^{68}Ga]Ga-FAPI-46-PET/CT over [^{18}F]-FDG-PET/CT in two.

By means of TBR we showed that tracer accumulation was significantly higher on [^{18}F]-FDG-[^{68}Ga]Ga-FAPI-46-PET/CT than on [^{18}F]-FDG-PET/CT in patients with HNT and esophageal cancer. Since the diagnostic performance of [^{68}Ga]Ga-FAPI-46-PET/CT has been shown to be best shortly after administration (*12*) and [^{18}F]-FDG-PET/CT is currently the gold standard, we recommend the injection of FAPI as a second tracer after the [^{18}F]-FDG-PET/CT-scan.

The main aim of developing this dual-tracer protocol is the better lesion detection with FAPI in less FDG-avid malignancies and higher TBR due to accumulation of both tracers in the malignant lesions. Limitations of this approach could be the failure to define exclusively FDG-positive lesions, diminished high sensitivity of FAPI-positive lesions in liver and brain hampered by FDG background and loss to evaluate metabolic response since SUVs are not measurable. Since it has been recently shown, that FAP can be also targeted with radioligand therapy in the animal model (*13*), the dual-tracer protocol would not allow a safe detection of FAP-expression as a theranostic approach.

In summary, the combined approach using two tracers for PET/CT imaging, enables patients to receive two PET/CTs with consecutively higher sensitivity within the same medical appointment.

Conclusion

We hereby introduce a practicable single session/dual-tracer protocol combining the strengths of two tracers without losing any diagnostic information relevant to cancer staging, as demonstrated by visual and semiquantitative assessment. We favor a protocol whereby a standard [^{18}F]-FDG-PET/CT is performed before the combined [^{18}F]-FDG-[^{68}Ga]Ga-FAPI-46-PET/CT within one appointment. Future studies may consider simultaneous injection of both tracers and acquisitions of just one single scan, to further simplify the procedure.

Acknowledgement

All authors declare that they have no conflicts of interest. This study did not receive any specific grant from funding agencies in the public, commercial, or not-for-profit sector.

Key points

QUESTION: Is combined assessment of single-tracer [^{18}F]-FDG-PET/CT and dual-tracer [^{18}F]-FDG-[^{68}Ga]Ga-FAPI-46-PET/CT within one appointment practical feasible and with a comparable diagnostic sensitivity compared to [^{18}F]-FDG-PET/CT alone?

PERTINENT FINDINGS: The retrospective study comparing the visual detection rate of suspicious lesions in single- and dual-tracer PET/CT showed equal results in four patients and superior lesion detection with dual-tracer PET/CT in two patients. Semiquantitative analyses of tumor to background ratios were significantly higher in dual-tracer than in single-tracer PET/CTs.

IMPLICATIONS FOR PATIENT CARE: Proofing practicability of single session/dual-tracer protocol allows combining the strengths of to complementary tracers with equal and in some cases superior diagnostic sensitivity for cancer staging.

References

1. Mathew S, Scanlan MJ, Mohan Raj BK, et al. The gene for fibroblast activation protein alpha (FAP), a putative cell surface-bound serine protease expressed in cancer stroma and wound healing, maps to chromosome band 2q23. *Genomics.* 1995;25:335-337.

2. Bauer S, Jendro MC, Wadle A, et al. Fibroblast activation protein is expressed by rheumatoid myofibroblast-like synoviocytes. *Arthritis Res Ther.* 2006;8:R171.

3. Wang XM, Yao TW, Nadvi NA, Osborne B, McCaughan GW, Gorrell MD. Fibroblast activation protein and chronic liver disease. *Front Biosci.* 2008;13:3168-3180.

4. Garin-Chesa P, Old LJ, Rettig WJ. Cell surface glycoprotein of reactive stromal fibroblasts as a potential antibody target in human epithelial cancers. *Proc Natl Acad Sci U S A.* 1990;87:7235-7239.

5. Kratochwil C, Flechsig P, Lindner T, et al. (68)Ga-FAPI PET/CT: Tracer Uptake in 28 Different Kinds of Cancer. *J Nucl Med.* 2019;60:801-805.

6. Meyer C, Dahlbom M, Lindner T, et al. Radiation Dosimetry and Biodistribution of (68)Ga-FAPI-46 PET Imaging in Cancer Patients. *J Nucl Med.* 2020;61:1171-1177.

7. Giesel FL, Kratochwil C, Lindner T, et al. (68)Ga-FAPI PET/CT: Biodistribution and Preliminary Dosimetry Estimate of 2 DOTA-Containing FAP-Targeting Agents in Patients with Various Cancers. *J Nucl Med.* 2019;60:386-392.

8. Ballal S, Yadav MP, Moon ES, et al. Biodistribution, pharmacokinetics, dosimetry of [(68)Ga]Ga-DOTA.SA.FAPi, and the head-to-head comparison with [(18)F]F-FDG PET/CT in patients with various cancers. *Eur J Nucl Med Mol Imaging.* 2021;48:1915-1931.

9. Giesel FL, Kratochwil C, Schlittenhardt J, et al. Head-to-head intra-individual comparison of biodistribution and tumor uptake of (68)Ga-FAPI and (18)F-FDG PET/CT in cancer patients. *Eur J Nucl Med Mol Imaging.* 2021.

10. Windisch P, Röhrich M, Regnery S, et al. Fibroblast Activation Protein (FAP) specific PET for advanced target volume delineation in glioblastoma. *Radiother Oncol.* 2020;150:159-163.

11. Shi X, Xing H, Yang X, et al. Fibroblast imaging of hepatic carcinoma with (68)Ga-FAPI-04 PET/CT: a pilot study in patients with suspected hepatic nodules. *Eur J Nucl Med Mol Imaging.* 2021;48:196-203.

12. Ferdinandus J, Kessler L, Hirmas N, et al. Equivalent tumor detection for early and late FAPI-46 PET acquisition. *Eur J Nucl Med Mol Imaging.* 2021.

13. Watabe T, Liu Y, Kaneda-Nakashima K, et al. Theranostics Targeting Fibroblast Activation Protein in the Tumor Stroma: 64Cu- and 225Ac-Labeled FAPI-04 in Pancreatic Cancer Xenograft Mouse Models. *Journal of Nuclear Medicine.* 2020;61:563.

Table 1: Patient characteristics, scan data and lesion detection with single versus dual-tracer PET/CT

Patients (n=6)	Mean;Standard deviation	Number of patients	
Age (years)	72.5 +/-12.3		
Sex		male 6; female 0	
Detected Malignant Findings on PET/CT		single-tracer	dual-tracer
Tumors (n=7)			
Oropharynx-CA		2	2
Cancer of Mouth Floor		1	1
Esophageal CA		4	4
Metastasis (n= 12)			
Lymph node metastasis			
- cervical		4	4
- mediastinal		1	**2 +**
- mesenterial		1	1
- retroperitoneal		1	1
- parailiacal		1	1
Pleural metastasis		1	1
Liver metastasis		1	**1 +**
Adrenal gland metastasis		1	1
PET/CT			
Time between FAPI injection and scan (min)	18.2; +/- 20.1		
Time between FDG and FAPI scan (min)	81.3 +/- 38.1		

+ indicates that more metastases were detected in the drainage area of mediastinal lymph nodes and liver on dual-tracer PET/CT than on single-tracer PET/CT

Table 2: Target to background ratios (TBRs) of count rates (CRs) measured in tumors, metastasis and background on [^{18}F]-FDG-[^{68}Ga]Ga-FAPI-46-PET/CT and [^{18}F]-FDG-PET/CT

TBR	[^{18}F]-FDG-[^{68}Ga]Ga-FAPI-46-PET/CT (Mean+/-SD)	[^{18}F]-FDG-PET/CT (Mean+/-SD)	Wilcoxon signed-rank test; Pearson`s correlation
$CR_{Tumor}/CR_{Background}$			
$CRpeak_T/CRmean_C$	3.7 +/- 1.7	1.8 +/- 1.0	z= -2.37, p= 0.008; r= 0.89
$CRpeak_T/CRmean_L$	8.0 +/- 4.1	4.7 +/- 2.3	z= -2.20, p= 0.016; r= 0.83
$CRpeak_T/CRmean_{BP}$	8.2 +/- 3.7	6.1 +/- 2.8	z= -2.20, p= 0.016; r= 0.83
$CRmax_T/CRmean_C$	4.3 +/- 1.8	2.1 +/-1.1	z= -2.37, p= 0.008; r= 0.89
$CRmax_T/CRmean_L$	9.3 +/- 4.2	5.7 +/- 2.6	z= -2.20, p= 0.016; r= 0.83
$CRmax_T/CRmean_{BP}$	9.5 +/- 3.7	7.3 +/- 3.2	z= -2.03 p= 0.023; r= 0.76
$CR_{Metastasis}/CR_{Background}$			
$CRpeak_M/CRmean_C$	2.2 +/- 1.2	0.8 +/- 0.5	z= -3.06, p≤ 0.001; r= 0.88
$CRpeak_M/CRmean_L$	2.9 +/- 1.0	1.9 +/- 1.0	z= -3.06, p≤ 0.001; r= 0.88
$CRpeak_M/CRmean_{BP}$	3.9 +/- 1.9	3.1 +/- 1.8	z= -2.51, p= 0.005; r= 0.72
$CRmax_M/CRmean_C$	2.9 +/- 1.6	1.1 +/- 0.6	z= -3.06, p≤ 0.001; r= 0.88
$CRmax_M/CRmean_L$	3.9 +/- 1.4	2.5 +/- 1.2	z= -2.82, p≤ 0.001; r= 0.81
$CRmax_M/CRmean_{BP}$	5.2 +/- 2.4	4.0 +/- 2.2	z= -2.35, p= 0.008; r= 0.68

CR_T:CR-tumor; CR_M:CR-metastasis; CR_C :CR-cerebellum; CR_L :CR-liver; CR_{BP} CR mediastinal blood pool

Figure Legends:

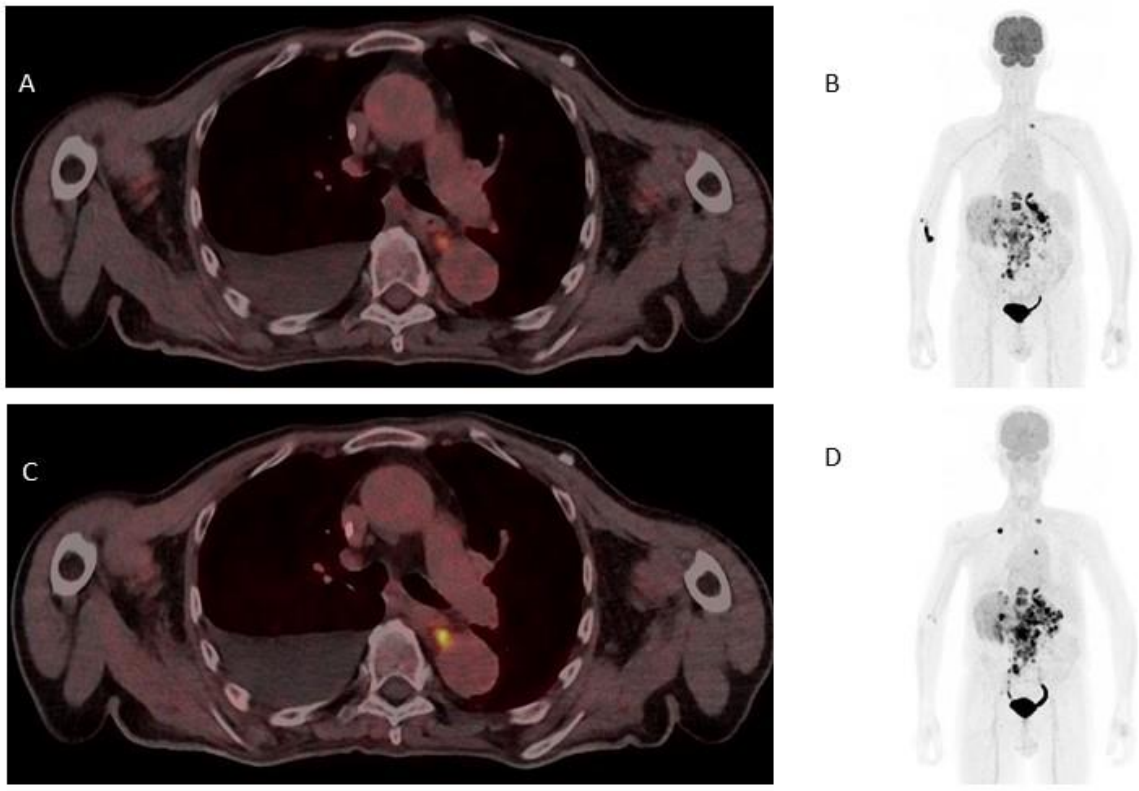

Figure 1: (A) Single-tracer PET/CT with [^{18}F]-FDG showing fused images in the axial plane of a primary tumor at the gastroesophageal junction with a metastasis in the left adrenal gland and liver metastases. (B) MIP of single-tracer PET images displaying high uptake in brain tissue, tracer accumulation around the injection side at the right elbow, lymph node (LN) metastasis in the left upper mediastinum, multiple abdominal LN metastases and liver metastases. An additional benign accumulation of FDG is visible, caused by right-sided thoracolumbar osteoarthritis. (C) Transverse section of fused dual-tracer [^{18}F]-FDG-[^{68}Ga]Ga-FAPI-46-PET/CT of the same patient as (A) and (B) with mediastinal LN metastasis. (D) As all images were visually normalized to the uptake of the liver, MIP of dual-tracer PET/CT in the same patient shows a less pronounced tracer accumulation in the brain tissue, compared to single-tracer PET/CT. In addition to lesions detected with single-tracer PET/CT, further abdominal LN metastasis and liver metastases are visualized via [^{18}F]-FDG-[^{68}Ga]Ga-FAPI-46-PET/CT. The focal tracer accumulation in the right vein angle is due to intravenous tracer accumulation from the former tracer depot at the right elbow.

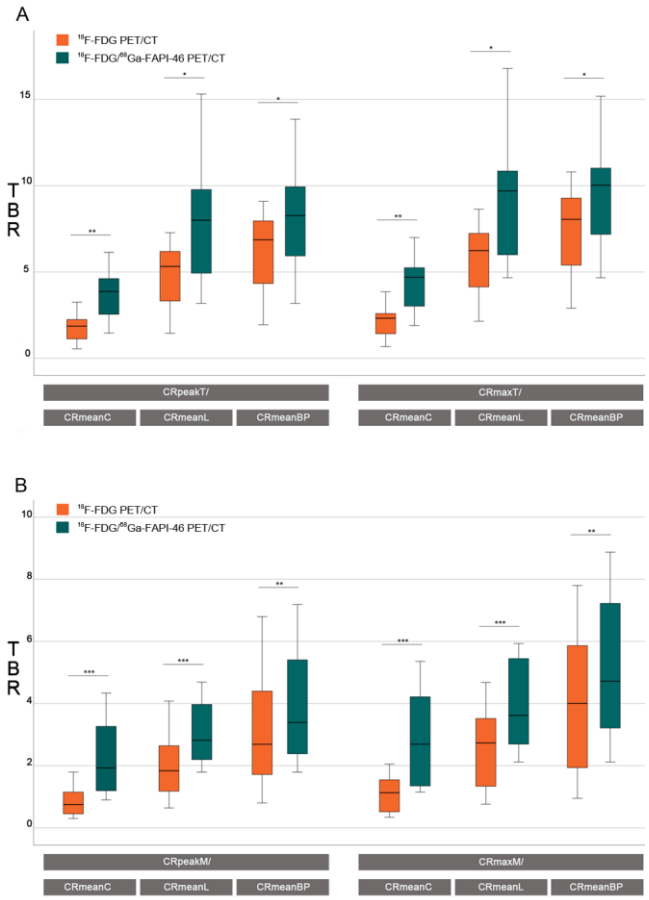

Figure 2: Boxplot of target to background ratios (TBRs) calculated from (A) CRpeak and CRmax of tumors (CRpeakT and CRmaxT) and (B) metastasis (CRpeakM and CRmaxM) versus CRmean of background (CRmeanCerebellum[CRmeanC], -Liver[CRmeanL] and -mediastinal blood pool[CRmeanBP]). The plots clearly display the tendency of median TBRs to be higher on dual-tracer [^{18}F]-FDG-[^{68}Ga]Ga-FAPI-46-PET/CT than on single-tracer [^{18}F]-FDG-PET/CT. These results were most obvious in TBRs of malignant tissue with cerebellum or liver as background.

Graphical Abstract: